

## Linear rate of grain growth in thin films during deposition

K. N. Tu,<sup>1</sup> A. M. Gusak,<sup>2</sup> and I. Sobchenko<sup>2</sup>

<sup>1</sup>*Department of Materials Science and Engineering, UCLA, Los Angeles, California 90095-1595*

<sup>2</sup>*Department of Theoretical Physics, Cherkasy State University, Cherkasy 18000, Ukraine*

(Received 26 June 2002; revised manuscript received 11 November 2002; published 10 June 2003)

Typical grain growth occurs in a polycrystalline phase under the constraint of constant volume, resulting in reduction of the total surface (grain boundary) area and energy. The grain growth rate is parabolic. We present here a different kind of grain growth in thin films during deposition, while the film is thickening. The grain growth rate can be linear. In vapor-phase deposition of face-centered-cubic metals such as Al and Cu, the grain size of the film is known to be nearly the same as the film thickness. A linear grain growth rate is expected if the deposition rate is constant. If we assume the grain size to be the same as the thickness, the total surface (grain boundary) area does not change. Under the constraint of a constant surface area, we present here a simple kinetic model of linear rate of grain growth during film deposition. We define it as flux-driven grain growth. A Monte Carlo simulation has been performed for comparison, and the results show a linear relationship between grain size and film thickness.

DOI: 10.1103/PhysRevB.67.245408

PACS number(s): 81.10.Bk, 64.70.Kb

### I. INTRODUCTION

In thin-film deposition, it is known experimentally<sup>1-4</sup> that the grain size in the film can be comparable to the film thickness. This is especially true for vapor deposition of face-centered-cubic metal films such as Al and noble metals on a fused quartz substrate at a few hundred degrees of centigrade. The thicker the film, the larger the grains. It indicates that the very process of deposition somehow enables grains to grow during deposition. The thickening of the film is accompanied by grain growth. It suggests a linear grain growth rate if the deposition rate is constant. It is very different from most of the known two-dimensional (2D) and 3D models of grain growth,<sup>5-10</sup> providing the parabolic time dependence for average grain size. In this linear mode of grain growth, if we assume the grain radius to be the same as the film thickness ( $r=H$ ), the total grain boundary area ( $S_{GB}$ ) remains constant during grain growth:

$$S_{GB} = N \times \frac{1}{2} 2 \pi r H = N \times \pi r^2 = S^{\text{substrate}} = \text{const.}$$

This is illustrated in Fig. 1, in which three sets of films of hexagonal grains with different grain size and thickness are shown on the same substrate area ( $S^{\text{substrate}}$ ). If we assume the edge of a hexagonal grain to be the same as the film thickness, the total grain boundary area in these three sets of film is the same. This is also true if we assume the grains to be cylindrical. Hence we have a unique case of grain growth in which the total surface area is constant but the volume increases. We define it as flux-driven grain growth (FDGG); it depends on the incoming atomic flux of deposition. This is quite different from the classical or normal grain growth in which the total volume of the grains is constant, but the grain boundary area decreases, and the grain growth rate is parabolic.

Recently, we developed a kinetic theory of ripening, flux-driven ripening (FDR), in which the ripening occurs under a constant surface area but growing volume. It is very different

from the classic Lifschitz-Slezov-Wagner (LSW) ripening wherein the ripening phase, under the constraint of a constant volume, reduces its surface area. The flux-driven ripening has been applied to the growth of scallop-type interfacial intermetallic compound of  $\text{Cu}_6\text{Sn}_5$  during the reaction between molten solder and copper.<sup>11</sup> If we assume the scallops are hemispheres, the total surface area between the melt and scallops is constant during the growth of the scallops. The driving force of flux-driven ripening is the gain of bulk Gibbs free energy of intermetallic compound formation in-

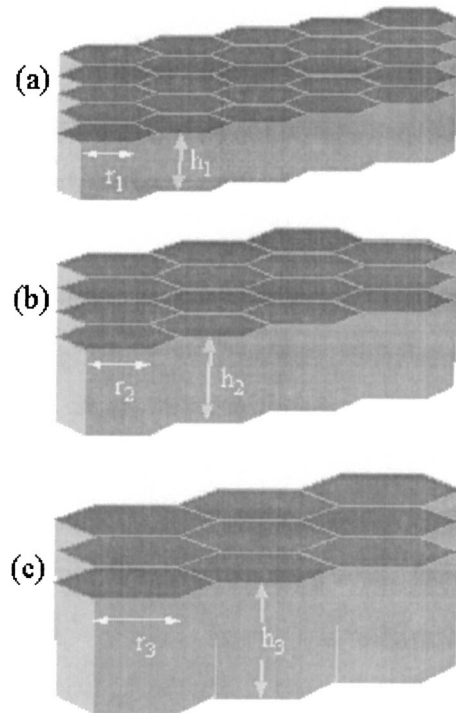


FIG. 1. Schematic diagram to illustrate the conservation of total surface of grain boundaries during grain growth in thin-film deposition.

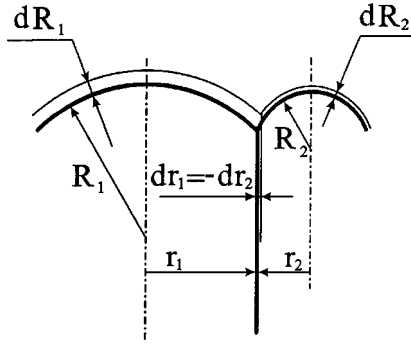


FIG. 2. Schematic diagram of the cross section of a pair of grains in thin-film deposition. The edge of the large grain will grow over the small grain due to the “mushroom effect.”

stead of the decrease of surface energy. Clearly, there is a strong similarity between flux-driven ripening and flux-driven grain growth; both of them are kinetic processes under the conditions of constant surface but growing volume.

## II. EDGE EFFECT ON THE SURFACE OF A PAIR OF GRAINS

In Fig. 2, the cross section of a pair of large (radius  $r_1$ ) and small (radius  $r_2$ ) neighboring grains is shown. The top surfaces of the grains are assumed to be spherical with radius  $R_1$  and  $R_2$ , respectively, and  $R_1 > R_2$ . We demonstrate below that the deposition flux enables the larger grain to grow by the so-called “edge or mushroom effect” and leads to a linear grain growth rate.

When atoms are being deposited onto the film surface, adatoms remain on the surface for some time, migrate on the surface, and are looking for suitable place to join the lattice of one of the grains. We suppose that the migration length of adatoms is very short, and they tend to attach to the “home” grain surface at the place of their “landing.” Furthermore, we suppose that the only place where a landing atom can choose its future “home” is in a narrow band in the vicinity of a junction where a grain boundary meets the surface. Denote the width of this band as  $2d$ , and take  $a \leq d < d_{\text{sink}}$ , where  $a$  is an interatomic distance, approximately equal to the spacing between atomic layers of the growing film,  $d_{\text{sink}}$  is a distance to nearest sink (surface step) for an adatom to join the lattice.

We suppose that each atom, landing onto this narrow band, inevitably chooses the larger grain as its “home” and joins the lattice of this grain with corresponding orientation. There will be atoms landed actually at the edge of the smaller grain inside the  $2d$  band, but they will join the lattice of the larger neighbor. It means that the larger grain will overlap its neighbor by a distance  $d$  during the building up of a new atomic layer, leading to a linear grain growth rate in proportion to the thickening rate.

The reason for an adatom to choose the larger grain is simply a larger average radius of this grain, hence the lower potential energy of corresponding sites. Difference of curvatures is not the only reason of choice. Difference of surface tensions of neighboring grains can well be a more powerful

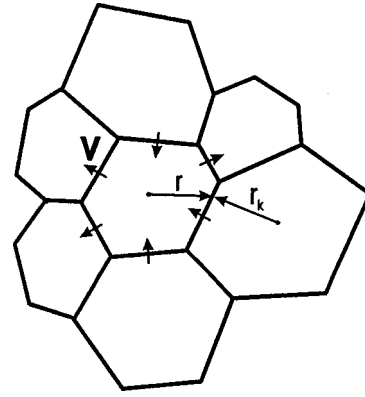


FIG. 3. Schematic diagram of the top view of grain growth during deposition. Velocities of all boundaries are the same in absolute value and directed from larger grain to smaller one.

factor, which is known as a reason of abnormal grain growth in the absence of the deposition flux. Here we do not take this factor into account explicitly. Yet it is obvious that during the initial stage of film formation or islands growth, those grains with less surface tension should grow faster, and after the formation of the initial layer, they start as the larger grains. Thus adatoms tend to choose them as their “home” grains.

In this simple model, the velocity of each grain boundary is the same,

$$V = \pm \frac{d}{\Delta t}, \quad (1)$$

where  $\Delta t$  is the time of one atomic layer deposition, which is determined by the flux density:

$$jS_t \Delta t = nS_t a, \quad (2)$$

where  $n$  is atomic density of the film and  $S_t$  is substrate or film surface area, so that

$$\Delta t = \frac{an}{j}, \quad V = \pm \frac{d}{a} \frac{j}{n}. \quad (3)$$

Hence the rate of film thickening is

$$\frac{dh}{dt} = \frac{a}{\Delta t} = \frac{j}{n} = \frac{a}{d} |V|. \quad (4)$$

Thus the velocity of grain boundary movement is approximately equal to the thickening rate and independent of the absolute value of the differences between the curvatures of  $R_1$  and  $R_2$ , as shown in Fig. 2. The direction of motion is always from the larger grain to the smaller grain.

## III. ANALYSIS OF FLUX-DRIVEN GRAIN GROWTH

In Fig. 3, let  $S$  be the top surface area of a certain grain with  $Z$  neighbors. Then

$$\frac{dS}{dt} = \sum_{k=1}^Z L_k V_k, \quad (5)$$

where  $L_k$  is the length of boundary with  $k$ th neighboring grain and  $V_k$  is its velocity, positive if  $S > S_k$  and negative if  $S < S_k$  (Fig. 3). Naturally, the smaller the neighboring grain, the shorter (in average) should be the length of boundary with it. We take simply that the grain size and the boundary length are proportional to each other:

$$L_k = qr_k, \quad (6)$$

where

$$r_k = \sqrt{S_k/\pi}.$$

On the other hand, the perimeter of the grain  $\sum_{k=1}^Z L_k$  can be approximated as  $2\pi r$  and  $r = \sqrt{S/\pi}$ . Thus,

$$q = \frac{2\pi r}{\sum r_k}, \quad L_k = 2\pi r \frac{r_k}{\sum_{i=1}^Z r_i}. \quad (7)$$

Substituting Eq. (7) into Eq. (5), one obtains

$$2\pi r \frac{dr}{dt} = 2\pi r \frac{\sum_{k=1}^Z r_k V_k}{\sum_{k=1}^Z r_k} \Rightarrow \frac{dr}{dt} = \frac{\frac{1}{Z} \sum_{k=1}^Z r_k V_k}{\frac{1}{Z} \sum_{k=1}^Z r_k},$$

$$V_k = \begin{cases} +|V|, & r_k < r, \\ -|V|, & r_k > r. \end{cases} \quad (8)$$

That is the basic equation for the growth or shrinkage of one arbitrary grain. It can be expressed in terms of a size distribution function if we neglect the ‘‘short-range order’’ effects:

$$\begin{aligned} \frac{dr}{dt} &= \frac{\langle r'V \rangle}{\langle r' \rangle} \\ &= \frac{\frac{1}{N} (\int_0^r r' |V| f(t, r') dr' + \int_r^\infty r' (-|V|) f(t, r') dr')}{\frac{1}{N} \int_0^\infty r' f(t, r') dr'}. \end{aligned} \quad (9)$$

[For a derivation of Eq. (9) in the frame of the mean-field approach, see the Appendix.]

Since a distribution function should obey a continuity equation, we have

$$\frac{\partial f}{\partial t} = -\frac{\partial}{\partial r} \left( f \frac{dr}{dt} \right) = -|V| \frac{\partial}{\partial r} \left[ f \left( 2 \frac{\int_0^r r' f(t, r') dr'}{\int_0^\infty r' f(t, r') dr'} - 1 \right) \right]. \quad (10)$$

Equation (10) indicates the possibility of  $r/t$  scaling. Indeed, we introduce the new variables

$$\begin{aligned} \tau = |V|t, \quad \xi = \frac{r}{|V|t} = \frac{r}{\tau} \Rightarrow \frac{\partial}{\partial t} &= |V| \left( \frac{\partial}{\partial \tau} - \frac{\xi}{\tau} \frac{\partial}{\partial \xi} \right), \\ \frac{\partial}{\partial r} &= \frac{1}{\tau} \frac{\partial}{\partial \xi}. \end{aligned} \quad (11)$$

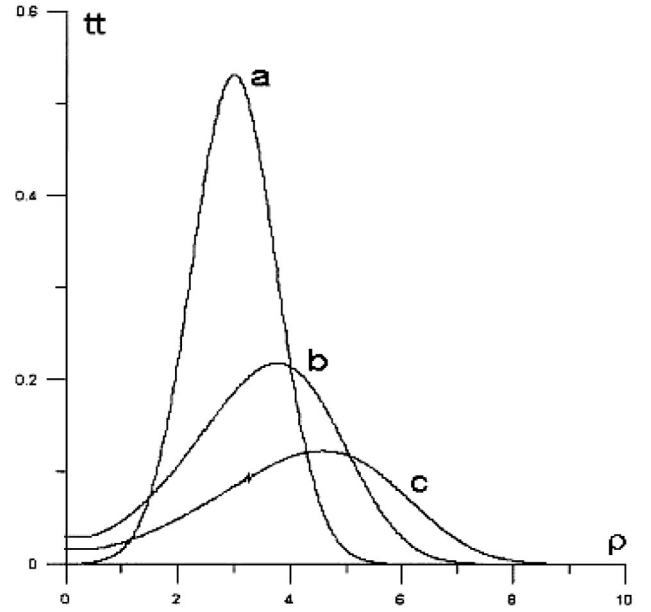


FIG. 4. Typical size distributions  $f(tt, \rho)$ , calculated according to Eq. (19). (a)  $tt=0$ , (b)  $tt=10$ , and (c)  $tt=20$ . Here  $\rho = r/L$ ,  $L = 2\gamma\Omega/kT$ , and  $tt = t, (d'/a)j'/nL$ .

Then Eq. (13) can be transformed into

$$\tau \frac{\partial f}{\partial \tau} = \xi \frac{\partial f}{\partial \xi} - \frac{\partial}{\partial \xi} \left[ f \left( 2 \frac{\int_0^\xi \xi' f(\tau, \xi') d\xi'}{\int_0^\infty \xi' f(\tau, \xi') d\xi'} - 1 \right) \right]. \quad (12)$$

A factorized solution is possible by taking

$$f(\tau, \xi) = g(\tau) \varphi(\xi). \quad (13)$$

Then,

$$\begin{aligned} \frac{d \ln g}{d \ln \tau} &= \frac{d \ln \varphi}{d \xi} \left( 1 + \xi - 2 \frac{\int_0^\xi \xi' \varphi(\xi') d\xi'}{\int_0^\infty \xi' \varphi(\xi') d\xi'} \right) - \frac{2\xi\varphi}{\int_0^\infty \xi' \varphi(\xi') d\xi'} \\ &= \lambda = \text{const}. \end{aligned} \quad (14)$$

We can determine the constant parameter  $\lambda$  from the constraint of conserving surface area:

$$\begin{aligned} \text{const} &= \int_0^\infty \pi R^2 f(t, R) dR \\ &= \pi g(\tau) \tau^3 \int_0^\infty \xi^2 \varphi(\xi) d\xi \Rightarrow g(\tau) = \text{const} \times \tau^{-3}. \end{aligned} \quad (15)$$

It leads to

$$\frac{d \ln g}{d \ln \tau} = \lambda = -3. \quad (16)$$

Equation (16) makes it possible to find the type of time dependence for the average grain size and for number of grains in the frame of our model:

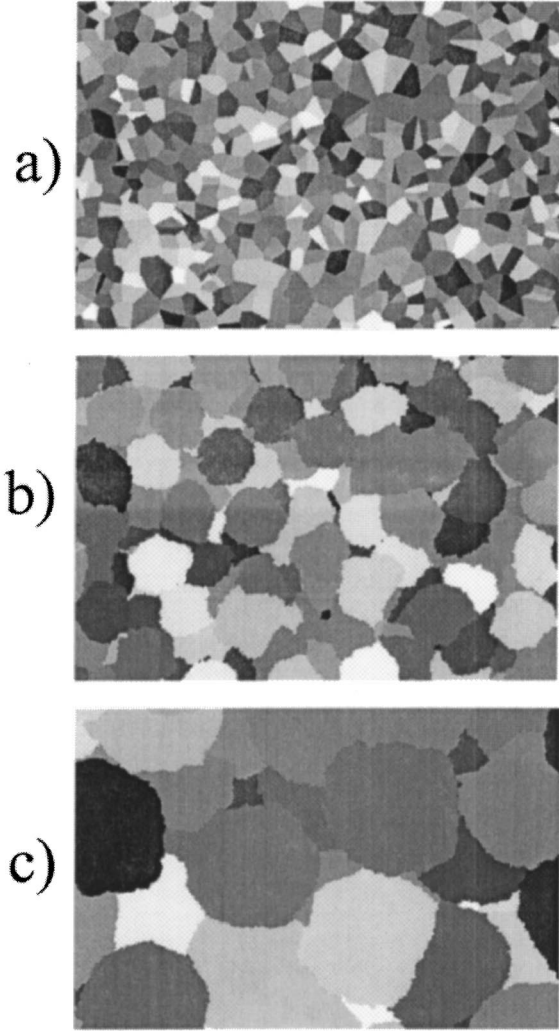


FIG. 5. Typical top views (fragments, 10% of total area) of grain structure evolution during deposition, obtained by Monte Carlo simulation: (a) initial distribution obtained as an areal array of Wigner-Seitz cells around randomly positioned centers, (b) after deposition of 100 atomic layers, and (c) after deposition of 300 layers.

$$\begin{aligned} \langle r \rangle &= \frac{\int_0^\infty r' f(t, r') dr'}{\int_0^\infty f(t, r') dr'} = \frac{\tau^2 g \int_0^\infty \xi' \varphi(\xi') d\xi'}{\tau g \int_0^\infty \varphi(\xi') d\xi'} \\ &= \langle \xi \rangle \tau = \text{const} |V| t, \\ N &= \tau g \int_0^\infty \varphi(\xi') d\xi' = \frac{\text{const}}{\tau^2}, \end{aligned} \quad (17)$$

Thus the average size in our model is indeed increasing linearly with time and, hence, it is proportional to the film thickness.

So far the choice of a “host” grain by adatoms within a narrow  $2d$  band around the surface area of a grain boundary was considered as totally deterministic: adatoms choose the larger grain, independent of difference of size of the two grains. It is physically evident that for a pair of grains having

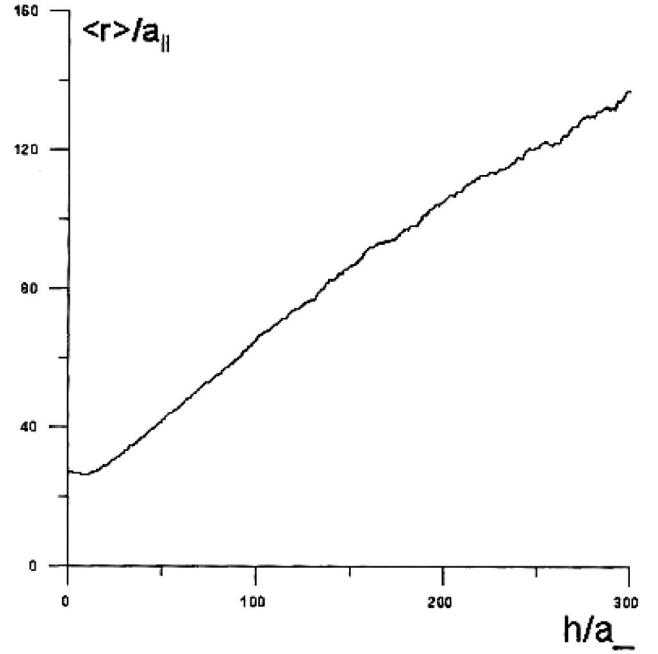


FIG. 6. Dependence of average grain size (in units of interatomic distance  $a_{\parallel}$ ) vs number of deposited layers ( $h$  is film thickness, and  $a_{\perp}$  is interlayer spacing), obtained by Monte Carlo simulation of flux-driven grain growth.

nearly the same size, the procedure could be stochastic. Therefore we use a Boltzmann distribution of probabilities between two neighboring grains, taking into account the energy difference as  $2\gamma\Omega(1/r_2 - 1/r_1)$ .

Then, instead of Eq. (3), the velocity of grain boundary between these two grains will be

$$V = \frac{d}{a} \frac{j}{n} \tanh \left[ \frac{2\gamma\Omega}{kT} \left( \frac{1}{r_2} - \frac{1}{r_1} \right) \right]. \quad (18)$$

This equation resembles the well-known Potts model<sup>12</sup> for normal grain growth, but deals only with adatoms arriving at the surface and choosing their host grain. In the mean-field approximation the corresponding equation for size distribution will have the following form:

$$\frac{\partial f}{\partial t} = - \frac{d}{a} \frac{j}{n} \frac{\partial}{\partial r} \left\{ f \tanh \left[ \frac{2\gamma\Omega}{kT} \left( \frac{1}{\langle r \rangle} - \frac{1}{r} \right) \right] \right\}. \quad (19)$$

Numerical solution of Eq. (19) has been made for non-dimensional time and space scales:  $\rho = r/L$ ,  $L = 2\gamma\Omega/kT$ ,  $tt = t(d/a)j/nL$ . The typical evolution of the size distribution from a Gaussian form presented initially is shown in Fig. 4. The time dependence of the average size appears to be almost linear.

#### IV. MONTE CARLO SIMULATION OF FLUX-DRIVEN GRAIN GROWTH

The above analytical and numeric results were checked by Monte Carlo simulations. A full Monte Carlo (MC) model taking into account the rate of deposition, diffusion of adatoms, their distribution among sinks leading to grain growth,

and possible changes of host grains at the free surface will be presented elsewhere. Here we present a simplified MC model, which almost directly corresponds to the above analytical model, with the following assumptions. (1) Only those atoms arriving at the surface near a grain boundary can choose their host grain. (2) If an atom arrived at the surface near a grain boundary and if it is above the larger grain, it inevitably chooses this larger grain as its host. (3) If an atom arrived at the surface near a grain boundary, but is above the smaller grain, it can nevertheless choose the larger grain as its host (edge effect) with probability  $p = pn$  ( $n = 0, 1, 2, 3$  in the case of square lattice), depending on the number of nearest-neighbor atoms of the smaller grain (excluding the atom just below).

Figure 5 demonstrates the typical top view of grain structure for the case  $p_3 = 0.1$ ,  $p_2 = 0.3$ , and  $p_1 = p_0 = 1$ . Figure 6 shows the average grain size (in units of interatomic distance) versus the number of deposited atomic layers. In full correspondence with the analytical model, the relation appears to be linear. (The initial nonmonotonic dependence is evidently due to random initial size distribution.) Moreover, the proportionality coefficient, obtained by numeric solution of Eq. (10) and calculation of  $\langle r \rangle$  versus  $h$ , appears to be 0.406, which is rather close to the MC result (0.390).

## V. SUMMARY

The linear rate of grain growth in thin-film deposition has been analyzed under the constraints of a constant rate of deposition and constant grain boundary area. Assuming that those adatoms deposited on the film surface near a grain boundary tend to choose the larger grain to grow, we have obtained a linear relationship between grain size and film

thickness. A Monte Carlo simulation has been performed and the results are in good agreement with the analysis.

## ACKNOWLEDGMENT

The project is supported by NSF Contract No. DMR-9987484.

## APPENDIX: PROOF OF THE EXPRESSION FOR THE AVERAGE GROWTH RATE IN FDGG

The growth rate of the area of an arbitrary grain is

$$\frac{dS}{dt} = \oint dl V(l). \quad (\text{A1})$$

The velocity of the grain boundary at interval  $dl$  is determined by the probabilities of this interval to be shared with a neighboring grain of size  $r'$ . First,  $f(r')dr'$  is the number of grains with sizes within the interval  $dr'$ . Then  $2\pi r'f(r')dr'$  is a length of boundaries of all these grains. The probability for certain boundary point to belong to this very class is a ratio of

$$\frac{\pi r' f(r') dr'}{\int \pi r' f(r') dr'} = p(r', r' + dr'). \quad (\text{A2})$$

Then the average velocity will be

$$\begin{aligned} V(l) &= \int V(r, r') p(r', r' + dr') \\ &= \frac{\int V(r, r') r' f(r') dr'}{\int r' f(r') dr'} = \frac{\langle r' V \rangle}{\langle r' \rangle}. \end{aligned} \quad (\text{A3})$$

<sup>1</sup>J. A. Thornton, *Annu. Rev. Mater. Sci.* **7**, 239 (1977).

<sup>2</sup>C. V. Thompson, *Annu. Rev. Mater. Sci.* **20**, 245 (1990).

<sup>3</sup>C. V. Thompson, *Solid State Phys.* **55**, 269 (2001).

<sup>4</sup>A. E. Lita and J. E. Sanchez, *J. Appl. Phys.* **85**, 876 (1999).

<sup>5</sup>J. E. Burke and D. Turnbull, *Prog. Met. Phys.* **3**, 220 (1952).

<sup>6</sup>M. Hillert, *Acta Metall.* **13**, 227 (1965).

<sup>7</sup>W. W. Mullins, *J. Appl. Phys.* **27**, 900 (1956).

<sup>8</sup>E. A. Holm, J. A. Glazier, D. J. Srolovitz, and G. S. Grest, *Phys. Rev. A* **43**, 2662 (1991).

<sup>9</sup>V. E. Fradkov, *Philos. Mag. Lett.* **58**, 271 (1988).

<sup>10</sup>M. Marder, *Phys. Rev. A* **36**, 438 (1987).

<sup>11</sup>A. M. Gusak and K. N. Tu, *Phys. Rev. B* **66**, 115403 (2002).

<sup>12</sup>E. A. Holm and C. C. Battaile, *JOM* **53**(9), 20 (2001).